

Research Article

Open Access



Efficient adsorptive removal of perfluorooctanoic acid by large surface area biochar modified with KHCO_3

Tao Hu^{1,2}, Jing-Qi Wu^{1,2}, Tong-Shuai Wang^{1,2,3}, Shi-Jia Li^{1,2}, Jia-Wei Chen^{1,2}

¹State Key Laboratory of Biogeology and Environmental Geology, China University of Geosciences, Beijing 100083, China.

²School of Earth Sciences and Resources, China University of Geosciences, Beijing 100083, China.

³China Household Electric Appliance Research Institute (CHEARI), Beijing 100053, China.

Correspondence to: Prof. Jia-Wei Chen, State Key Laboratory of Biogeology and Environmental Geology, China University of Geosciences, Xueyuan Road 29, Haidian, Beijing 100083, China. E-mail: chenjiawei@cugb.edu.cn

How to cite this article: Hu, T.; Wu, J. Q.; Wang, T. S.; Li, S. J.; Chen, J. W. Efficient adsorptive removal of perfluorooctanoic acid by large surface area biochar modified with KHCO_3 . *Water Emerg. Contam. Nanoplastics* 2025, 4, 9. <https://dx.doi.org/10.20517/wecn.2025.01>

Received: 4 Jan 2025 **First Decision:** 26 Feb 2025 **Revised:** 3 Mar 2025 **Accepted:** 13 Mar 2025 **Published:** 24 Mar 2025

Academic Editor: Joana C Prata **Copy Editor:** Pei-Yun Wang **Production Editor:** Pei-Yun Wang

Abstract

Biochar is a promising adsorbent for remediating perfluorooctanoic acid (PFOA) in contaminated water. However, the performance of pristine biochar is limited. Considering pore filling is a crucial mechanism for PFOA adsorption on biochar, this study investigated the impact of KHCO_3 modification on the pore structure of biochar and its adsorption capacity for PFOA. The characterization and experiment results revealed that both the specific surface area (SSA) and adsorption capacity of biochars were positively correlated with the pyrolysis temperature, and modified corn stalks biochar prepared at 800 °C (CBC-800) exhibited a noticeable SSA (1,471.6 m^2/g) and adsorption capacity (514.8 mg/g), which were 3.6 and 37.1 times higher, respectively, compared to pristine corn stalk biochar (404.1 m^2/g and 13.9 mg/g). The adsorption kinetics and the isotherm data followed pseudo-second-order kinetics and the Freundlich model, respectively, indicating chemisorption was the main factor limiting the adsorption rate. Thermodynamics demonstrated the adsorption process was physical, spontaneous, and exothermic. The porous biochars performed superior adsorption capacities under various environmental conditions (pH, inorganic salts, etc.). The removal rate of CBC-800 for low concentrations of PFOA (10-1,000 $\mu\text{g}/\text{g}$) ranged from 87.4% to 99.6%, and this rate was positively correlated with the initial concentrations. Additionally, CBC-800 effectively removed PFOA (40 $\mu\text{g}/\text{L}$) through six consecutive adsorption cycles (93.4%-94.5%). Mechanism



© The Author(s) 2025. **Open Access** This article is licensed under a Creative Commons Attribution 4.0 International License (<https://creativecommons.org/licenses/by/4.0/>), which permits unrestricted use, sharing, adaptation, distribution and reproduction in any medium or format, for any purpose, even commercially, as long as you give appropriate credit to the original author(s) and the source, provide a link to the Creative Commons license, and indicate if changes were made.



analysis indicated dominant pore filling was greatly enhanced, while hydrogen bonding, electrostatic, and hydrophobic interactions were also involved. Our study demonstrated that biochar derived from low-cost agricultural and forestry residues combining KHCO_3 modification has great potential for the adsorptive removal of emerging PFAS in contaminated water.

Keywords: Biochar, KHCO_3 modification, PFOA, pore filling, adsorption

INTRODUCTION

Perfluorooctanoic acid (PFOA) is a synthetic perfluoroalkyl substance (PFAS) that has distinctive properties such as hydrophilic and lipophilic characteristics, attributed to its unique amphiphilic structure consisting of a hydrophilic carboxyl head and a hydrophobic perfluoro tail^[1,2]. It is extensively utilized in numerous products, including food contact paper, firefighting foam, non-stick cookware, and industrial antifouling agents^[3,4]. Due to the pervasive use of these products, PFOA has been widely detected in a variety of environmental media, including municipal sewage and underground water^[5,6]. The C–F bond of PFOA possesses a bond energy of about 530 kJ/mol, providing remarkable stability and rendering it resistant to environmental degradation^[7]. PFOA has been found to have an increased risk of cardiovascular, respiratory, and neurological disease^[8]. Due to growing concerns over the environmental (especially the water system) and health risks posed by PFOA, it is classified as an “emerging contaminant”. As a result, there is significant public concern regarding the remediation of PFOA-contaminated water.

Various technologies have been employed to eliminate PFOA from water, including membrane separation, adsorption, advanced oxidation processes, electrochemical degradation, photochemical degradation, *etc.*^[2,9,10]. Among these, electrochemical and photochemical methods have obtained a lot of attention due to their high efficiency in degrading PFOA contaminants in aqueous environments. However, these methods often require additional energy input and specialized conditions, which may limit their practical application in certain scenarios. Adsorption is a promising technology due to its environmental friendliness, ease of operation, and renewability^[11]. Biochar can serve as an attractive adsorbent with regulable physiochemical properties, abundant forestry and agricultural residues, simple preparation processes, and renewability^[12,13]. However, conventional biochars have limited adsorption sites, a low specific surface area (SSA), and porosity, making it difficult to efficiently remove PFOA^[14]. It has been documented that the porosity of the adsorbents plays a critical factor in the adsorption of PFAS^[15,16]. Therefore, improving the pore structure of biochar could effectively enhance its adsorption capacity for PFOA. Currently, the predominant methods to increase the SSA of biochars involve chemical modification. For instance, Fagbayigbo *et al.* prepared grape leaf biochar at 900 °C and activated it with H_3PO_4 , achieving a maximum adsorption capacity (Q_m) of 78.9 mg/g for PFOA^[17]. Similarly, Deng *et al.* utilized KOH modification to produce bamboo-derived biochar at 900 °C, resulting in a Q_m of 476.2 mg/g for PFOA^[18]. However, such modification processes may cause secondary pollution and equipment corrosion, underscoring the need for a more sustainable and efficient modification method.

Modification with KHCO_3 , as a mild and non-corrosive modification method, can increase biochar adsorption capacities for pollutants by improving the pore structure^[19]. For instance, Wang *et al.* indicated that KHCO_3 -modified biochar pyrolyzed at 900 °C (PBC-900) exhibited a remarkably larger SSA (2,017.6 m^2/g) compared to PBC-500 (162.3 m^2/g)^[20]. Moreover, the maximum adsorption capacity of PBC-900 for benzo(a)pyrene was enhanced by 6 times. Similarly, Ma *et al.* utilized KHCO_3 as an activator to rapidly pyrolyze various biomasses, obtaining a variety of biochars to evaluate the impact of biomass types on methylene blue adsorption^[21]. The results revealed that biochar derived from corn stalks achieved a

remarkable 99.9% removal rate, markedly outperforming wheat straw biochar (52.6%). The aforementioned studies showed that the choice of biomass and pyrolysis temperature significantly influence the physicochemical properties of biochar, which are crucial for its adsorption capabilities. Therefore, carefully selecting the appropriate pyrolysis temperature and biomass is essential to enhancing the adsorption performance of biochar towards PFOA through environmentally friendly modifications.

In this study, pine sawdust and corn stalks were chosen as biochar precursors owing to their widespread availability and representation of cellulose and lignin biomass^[22], respectively. The porous biochar was prepared via KHCO_3 modification and used for PFOA adsorption. The following were the study's aims: (1) preparation and characterization of porous biochars obtained from different pyrolysis temperatures and biomass using KHCO_3 modification; (2) comparison of PFOA adsorption on different obtained biochars; and (3) elucidation of the underlying mechanism for the enhancement of PFOA adsorption on porous biochar. This study used KHCO_3 modification to enhance the adsorption capacity of biochars derived from widely available biomass, providing valuable insights into the development of sustainable and efficient materials for the removal of PFOA from contaminated water.

MATERIAL AND METHODS

Chemicals

PFOA ($\text{C}_8\text{HF}_{15}\text{O}_2$), potassium hydrogen carbonate (KHCO_3), sodium hydroxide (NaOH), and ethyl alcohol (EtOH) were supplied from Macklin Biochemical (Shanghai, China). Hydrochloric acid (HCl), sodium chloride (NaCl), and calcium chloride (CaCl_2) were obtained from Sinopharm Group Chemical Reagent (Beijing, China). Acetonitrile and methanol were all HPLC quality from ANPEL Laboratory Technologies (Shanghai, China). Sodium dihydrogen phosphate (NaH_2PO_4) was obtained from Beijing Reagent (Beijing, China). Deionized water (DIW , $> 18.25 \text{ M}\Omega\text{-cm}$) was used during experiments. More information can be found in the [Supplementary Table 1](#).

Preparation of biochar

After washing and drying the biomass corn stalks and pine sawdust, a 100-200 mesh screen was used to sift the biomass powder. The biomass powders and KHCO_3 were magnetically stirred in a beaker containing DIW at a mass ratio of 2:1 for 1 h before being dried in an oven at 80°C . Next, the mixtures were placed in a corundum boat and maintained for 2 h in a tubular furnace at the desired temperature, such as 600, 700, and 800°C , with a heating rate of $5^\circ\text{C}/\text{min}$. The pyrolysis temperature and the ratio of KHCO_3 to biomass were selected according to the pre-experiment [[Supplementary Figure 1](#)]. After natural cooling to room temperature, the solid products were rinsed with 0.1 M HCl and DIW until the pH of the filtrate was neutral before being dried in an oven. The resulting modified pine sawdust and corn stalks biochar were denoted as PBC-T and CBC-T, respectively, where T represents the pyrolysis temperatures.

Characterization of biochar

The morphologies of porous biochars were observed by scanning electron microscopy (SEM, Zeiss Supra 55-VP). The pore structure of porous biochars was analyzed using the Brunauer-Emmett-Teller method (BET, QuadraSorb Station 1 analyzer). Biochars were heated for 4 h at 750°C in a muffle furnace in order to measure their ash content. The functional groups of porous biochars were identified by Fourier transform infrared spectroscopy (FTIR, Nicolet iS10 spectrometer). The content of elements in porous biochars was obtained by an elemental analyzer (Euro Vector EA300), and the O content was inferred from the residual mass of these elements and ash content. The graphitization degree and defects of porous biochars were analyzed by Raman spectra (inVia Reflex, UK). This study used a zeta potential analyzer to measure the zeta potential of porous biochars (NanoBrook Omni).

Adsorption experiments

The PFOA solution was configured with 10 mM NaCl as the background solution, and 0.1 M HCl and NaOH were used to adjust the pH to 7 ± 0.2 . Biochars (0.2 g/L) were added to glass bottles containing 50 mg/L PFOA solution for adsorption kinetics experiments and shaken at 25 °C and 180 rpm for two days to reach equilibrium. At certain time intervals, 1 mL of supernatant was extracted and filtered through a 0.45 μ m polyether sulfone filter into a brown vial to quantify the PFOA concentration.

For adsorption thermodynamics, an accurate 10 mg of biochar was added to glass bottles containing 50 mL of PFOA solution at a range of concentrations (30, 50, 80, 120, 160, 200, and 240 mg/L) and shaken in a shaker at desired temperatures (15, 25, 35 °C) at 180 rpm for 1 day. After equilibrium, the supernatant was extracted to quantify the PFOA concentration. In addition, the desorption experiments were performed immediately after adsorption reached equilibrium. Specifically, the liquid in the centrifugal tube was carefully removed, and different desorption solutions (DI water, 0.5 M NaOH, and 25%-95% ethanol) were added, and the PFOA concentration was determined after shaking for 48 h. The pH effect experiments on PFOA adsorption by biochar were investigated by changing the initial pH (3, 5, 7, 9, 11) of the solution. The influence of co-existing ions was compared by changing the concentrations of NaCl, CaCl₂, NaNO₃, and Na₂SO₄ (0, 5, 25, and 50 mM, respectively).

To further assess the PFOA removal efficiency of CBC-800 at low concentrations, CBC-800 (0.2 g/L) was added into a glass bottle containing 50 mL of PFOA solutions at concentrations ranging from 0.01 to 1 mg/L. After 24 h, the supernatant was extracted to quantify the PFOA concentration. For the recycling experiment, 0.2 g/L of CBC-800 was added to a centrifuge tube containing 50 mL of PFOA solution (40 μ g/L), and the supernatant was sampled after 24 h to quantify the PFOA concentration. Subsequently, the solution in the centrifuge tube was replaced with 50 mL of fresh PFOA solution (40 μ g/L), and the adsorption process was repeated for six consecutive cycles to evaluate the long-term adsorption performance of CBC-800. All the experiments were conducted in triplicate.

PFOA analysis

The PFOA was quantitatively measured according to our previous study^[23]. Briefly, the concentration of PFOA was quantified by HPLC (Shimadzu LC-20 A, Kyoto, Japan) equipped with a C18 column (250 mm \times 4.6 mm, 5 μ m). The iso-volumetric elution of acetonitrile/20 mM NaH₂PO₄ (50/50, v/v) (pH 2) was performed at a flow rate of 1 mL/min with an injection volume of 25 μ L, and the UV wavelength was 210 nm.

RESULTS AND DISCUSSION

Characterization of biochar

The microscopic morphologies of biochars are shown in [Supplementary Figure 2](#). Both pine sawdust-modified biochars (PBC) and corn stalks-modified biochars (CBC) exhibited abundant etched pits and well-developed pore structures on their surfaces, indicating that the porous structures of biochars were largely improved after being activated with KHCO₃, as evidenced by the comparison with the pristine corn stalk biochar in our previous study^[23]. Additionally, biochars produced at higher pyrolysis temperatures displayed more intensive pits. This can be attributed to the decomposition of KHCO₃ into K and K₂O at high temperatures, with the K and K₂O embedded in biochar promoting the formation of micropores [Equations (1)-(4)]^[24]. As pyrolysis temperature increased, the decomposition rate of KHCO₃ accelerated, leading to a more thorough decomposition and consequently a larger SSA. This enhancement in SSA was favorable for the efficient transport of PFOA.



To further clarify the pore structure of porous biochars, the N_2 adsorption/desorption curve was conducted, and the results were presented in Table 1 and Figure 1. The S_{BET} of PBC and CBC increased significantly with the pyrolysis temperature, from 672.38 to 1,253.46 m^2/g for PBC, and from to 1,471.6 m^2/g for CBC, when the pyrolysis temperature was raised from 600 to 800 $^{\circ}\text{C}$. Notably, the S_{BET} of CBC-800 obviously exceeded that of the corn stalk biochar (404.10 m^2/g) reported in our previous study^[23]. This increase in S_{BET} could be attributed to the reaction between KHCO_3 and biochar, resulting in the formation of K and K_2O , which become embedded in the biochar and promote the formation of micropores^[25]. Furthermore, at the same pyrolysis temperature, CBC exhibited a higher SSA than PBC due to its higher content of cellulose^[26].

The elemental analysis data and ash content for porous biochars are presented in Table 2. It was found that the ash content of PBC was lower than that of CBC, which could be attributed to the difference in the cellulose content of biomass. The atomic ratios analysis could indicate the aromatics and polarity of porous biochars^[27]. The atomic ratio of H/C for PBC and CBC decreased from 0.219 to 0.065 and 0.141 to 0.048, respectively, demonstrating the enhancement in the aromaticity of porous biochars as the pyrolysis temperatures increased from 600 to 800 $^{\circ}\text{C}$. Moreover, the aromaticity of CBC-800 was notably higher than that of the other biochars, suggesting that CBC-800 was favored for adsorbing aromatic pollutants. Based on Table 2, the analogous O/C and (O + N)/C atomic ratios of PBC (0.055-0.075 and 0.064-0.084) and CBC (0.058-0.154 and 0.072-0.168) indicated the porous biochars possessed similar hydrophilicity.

To further investigate the defects and the graphitization degree of biochars, Raman spectra were characterized, as shown in Figure 2. The $I_{\text{D}}/I_{\text{G}}$ ratio could measure the graphite defects of porous biochars^[16]. The $I_{\text{D}}/I_{\text{G}}$ ratio of CBC (0.98-1.01) was obviously higher than PBC (0.90-0.99), indicating that CBC possessed more graphite defects. Both PBC and CBC showed an increase in the $I_{\text{D}}/I_{\text{G}}$ ratio with increasing pyrolysis temperature, from 0.90 to 0.99 for PBC and 0.98 to 1.01 for CBC. This suggested that higher pyrolysis temperature contributed to the formation of graphite defects in biochars, which may explain the observed increase in S_{BET} and pore formation. The graphite defects in the pores of porous biochars can provide rapid diffusion channels for the organic compounds, thereby promoting the adsorption of organic compounds^[28].

Biochar had a lot of functional groups that played a critical role in the adsorption of organic pollutants^[29]. The FTIR spectra of the porous biochars before adsorption of PFOA was shown in Supplementary Figure 3A. Typical functional groups exhibited large absorption peaks on the spectrum, such as -OH and $-\text{CH}_x$ stretching vibration at 3,483 cm^{-1} and 2,822-2,971 cm^{-1} , respectively. In addition, the absorption peaks of C-O-C and C=C were observed at 1,097 and 1,573 cm^{-1} , respectively^[30]. Despite variations in biomass types and pyrolysis temperatures, the functional groups of the porous biochars showed minimal differences.

PFOA adsorption

The adsorption kinetics could reflect the rate at which adsorbates were adsorbed on the adsorbents, providing valuable information such as the kinetic adsorption constant. The adsorption kinetics of biochars

Table 1. Physical properties of porous biochars

Biochars	S_{BET}^a (m ² /g)	S_{mic}^b (m ² /g)	S_{mes}^c (m ² /g)	V_{total}^d (cm ³ /g)	V_{mic}^e (cm ³ /g)	Ave-pore diameter (nm)
PBC-600	672.39	619.99	52.39	0.32	0.25	1.92
PBC-700	955.89	892.73	63.14	0.51	0.42	2.15
PBC-800	1,253.46	1,173.81	79.65	0.60	0.49	1.91
CBC-600	765.48	672.91	92.56	0.42	0.28	2.17
CBC-700	1,197.19	1,015.54	181.65	0.81	0.57	2.71
CBC-800	1,471.64	1,361.86	109.78	0.81	0.62	2.20

^a S_{BET} is the SSA analyzed by BET method. ^b S_{mic} is the microporous surface area. ^c S_{mes} is the mesoporous surface area by the t-plot method external surface area ($S_{\text{mes}} = S_{\text{BET}} - S_{\text{mic}}$). ^d V_{total} is the total volume acquired at $P/P_0 = 0.99$. ^e V_{mic} is the microporous pore volume and calculated by t-plot method. BET: Brunauer-Emmett-Teller; PBC: pine sawdust-modified biochars; CBC: corn stalks-modified biochars; SSA: specific surface area.

Table 2. Elemental composition, atomic ratio, ash content and yield of biochars

Biochars	Element content (%)					Atomic ratio			Ash content (%)	Yield (%)
	C	H	N	S	O	H/C	O/C	(O + N)/C		
PBC-600	90.09	1.65	0.89	0.22	6.61	0.219	0.055	0.064	0.54	20.53
PBC-700	88.70	0.89	0.88	0.25	8.92	0.121	0.075	0.084	0.36	13.71
PBC-800	89.35	0.49	1.08	0.24	7.68	0.065	0.064	0.075	1.16	12.72
CBC-600	84.18	0.99	1.03	0.15	12.07	0.141	0.108	0.118	1.58	21.45
CBC-700	78.63	0.91	1.22	0.24	16.20	0.139	0.154	0.168	2.80	14.87
CBC-800	86.17	0.35	1.42	0.27	6.69	0.048	0.058	0.072	5.10	10.04

PBC: Pine sawdust-modified biochars; CBC: corn stalks-modified biochars.

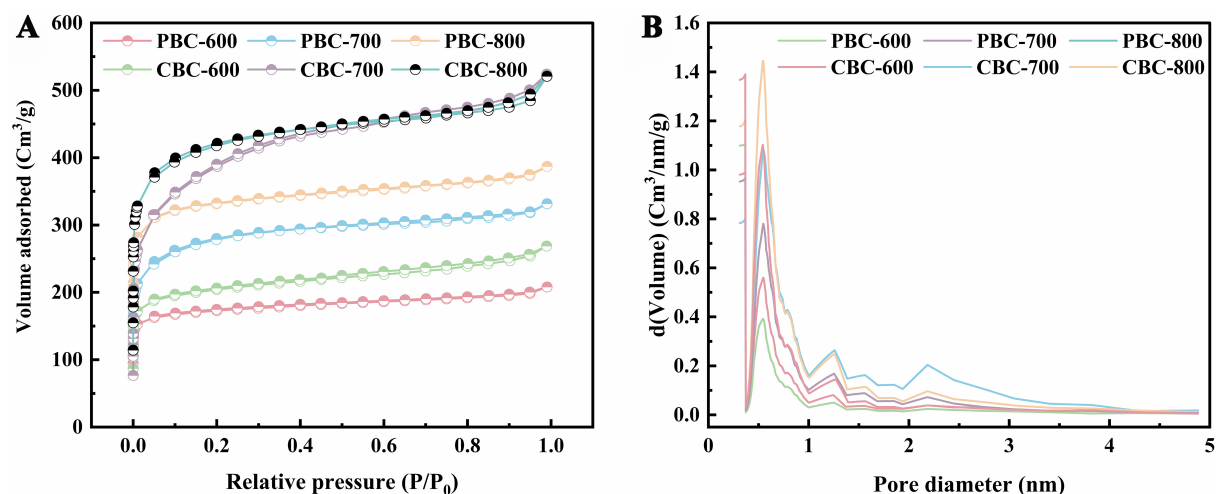


Figure 1. (A) N₂ adsorption-desorption isotherm of biochars and (B) pore size distribution curve measured by BJH method. BJH: Barrett-Joyner-Halenda.

for PFOA are shown in Figure 3A and B. It was observed that different biochars exhibited a similar trend in PFOA adsorption, with rapid PFOA removal occurring within the initial 60 min due to the abundance of active sites on their surfaces, facilitating swift uptake. Subsequently, as these sites were occupied, the adsorption rate gradually decreased until equilibrium was reached. Therefore, the PFOA adsorption process can be divided into distinct phases: an initial phase characterized by rapid adsorption (0-1 h) and a slower phase (1-24 h). The adsorption kinetics data for the porous biochars were fitted to the kinetic models, and

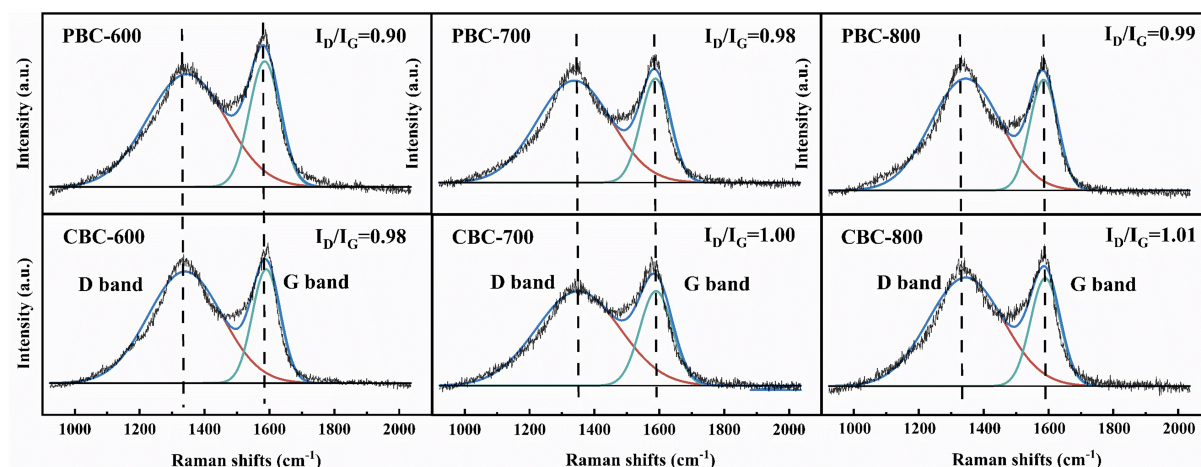


Figure 2. Raman spectra of porous biochars.

the kinetic constants were shown in [Supplementary Table 2](#). From the correlation coefficient (R^2) in [Supplementary Table 2](#), compared with the pseudo-first-order kinetic model (0.891-0.958), both the pseudo-second-order kinetic model (0.963-0.993) and the Elovich model (0.963-0.985) showed better fits. Furthermore, the experiment data better fitted the pseudo-second-order kinetic model, suggesting that chemisorption was the rate-limiting stage of biochar adsorption^[31,32]. The α value of the Elovich model exceeded β , indicating a faster adsorption rate compared to the desorption process, suggesting a strong affinity between the PFOA and the adsorbent^[33].

The maximal adsorption capacities of porous biochars were evaluated through the adsorption isotherm. The experiment data were fitted to the Langmuir and Freundlich models [[Figure 3C and D](#)], and the parameters obtained from these models offer valuable insights into the adsorption mechanism. According to the R^2 in [Supplementary Table 3](#), PFOA adsorption on porous biochars prepared at pyrolysis temperatures of 700 and 800 °C showed a better fit to the Freundlich model (0.969-0.995) than the Langmuir model (0.837-0.920), indicating the presence of multilayer adsorption^[34]. The Langmuir and Freundlich models are based on the assumption of homogeneous and heterogeneous adsorbent surfaces, respectively. The Raman spectra of porous biochars possessed high enough D bands [[Figure 2](#)], suggesting the existence of heterogeneous surface sites, which was consistent with the model fitting results. In the Langmuir model, the adsorption affinity coefficient (K_L) was obtained, with CBC-800 exhibiting a higher K_L value (0.14) compared to other biochars (0.04-0.08). This suggested a stronger binding affinity between CBC-800 and PFOA^[35]. In the Freundlich model, the n of porous biochars (0.26-0.35) indicated nonlinear sorption isotherms. The maximal adsorption capacities of porous biochars were significantly impacted by the pyrolysis temperatures. Specifically, PBC-800 and CBC-800 displayed impressive adsorption performance of 440.3 and 514.8 mg/g, respectively, whereas CBC-600, PBC-700, and CBC-700 exhibited lower adsorption capacities ranging from 82.1 to 239.7 mg/g. Notably, CBC-800 demonstrated exceptional adsorption performance (514.8 mg/g) compared to other adsorbents, such as unmodified corn stalks biochar (13.9 mg/g), polyethyleneimine modified graphene oxide (10.1 mg/g), magnetic activated carbon (372.6 mg/g), etc. [[Supplementary Table 4](#)]. The superior PFOA adsorption performance of CBC-800 highlighted that KHCO_3 modification was an efficient approach for enhancing the adsorption capacities of biochars for the removal of PFOA from contaminated water.

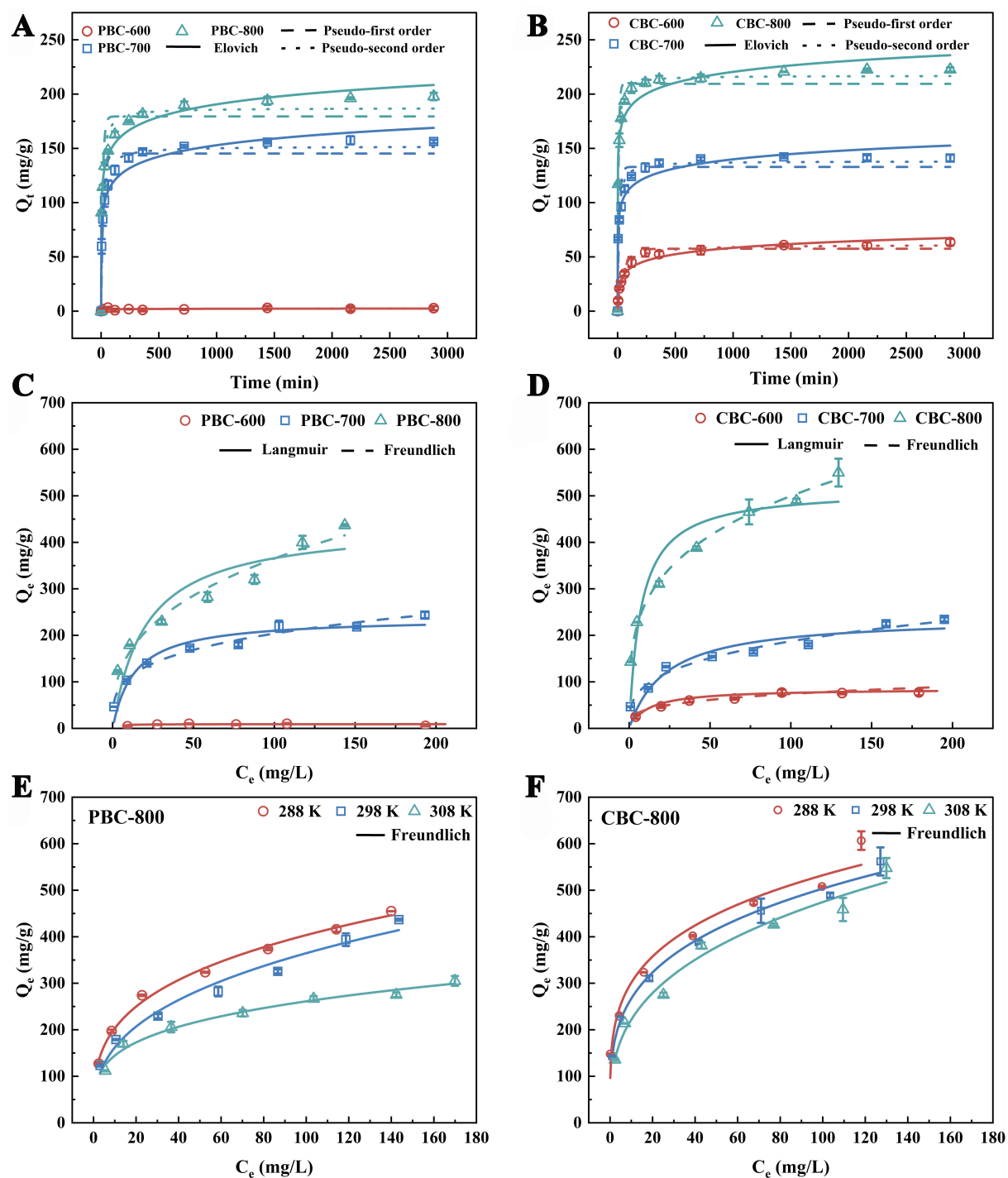


Figure 3. (A and B) Adsorption kinetics; (C and D) adsorption isotherms of biochars for PFOA; and (E and F) adsorption thermodynamics of PBC-800 and CBC-800 for PFOA. PFOA: Perfluorooctanoic acid; PBC: pine sawdust-modified biochars; CBC: corn stalks-modified biochars.

Furthermore, to investigate the spontaneity of biochar adsorption of PFOA, the superior adsorption capacities of CBC-800 and PBC-800 were selected for adsorption thermodynamics analysis [Figure 3E and F]. It was shown that the adsorption capacity at equilibrium decreased with increasing temperature, indicating that higher temperatures could have a certain inhibitory impact on the biochar

adsorption process. This could be due to the increased movement frequency of PFOA in solution at higher temperatures, making it less susceptible to being bound by the pores of biochar^[36]. By calculating the parameters of the thermodynamic formula, the adsorption behavior and mechanism were discussed. The thermodynamic formulas for parameter calculation are presented in [Supplementary Text 1](#).

The obtained thermodynamic parameters are shown in [Table 3](#). Within the temperature range of 298–318 K, all ΔG^0 values (–10.59 to –12.30 kJ/mol) were negative, confirming that the adsorption processes were spontaneous^[37]. In addition, the negative ΔH^0 values (–9.20 and –18.30 kJ/mol) for PBC-800 and CBC-800 indicated that the adsorption process was exothermic^[38]. The negative ΔG^0 and ΔH^0 values for both PBC-800 and CBC-800 represented that the adsorption was dominated by physical adsorption^[39]. The parameter ΔS^0 could quantify the degree of disorder during the biochar adsorption process. The positive ΔS^0 values (5.92 J·mol^{–1}·K^{–1}) for PBC-800 indicated the PFOA adsorbed on biochar was still free to move^[40]. In contrast, the negative ΔS^0 values (–20.61 J·mol^{–1}·K^{–1}) for CBC-800 showed a strong interaction between PFOA and CBC-800, indicating that PFOA was more tightly bound to the surface of CBC-800.

The ionization degree of PFOA molecules and the charge of the biochars were impacted by the pH of the solution^[41]. The influence of pH on porous biochar adsorption performances is illustrated in [Figure 4A](#). It was shown that the PFOA adsorption capacity of CBC-800 (244.8 mg/g) and PBC-800 (240.6 mg/g) was optimal at pH 3, with adsorption gradually declining as pH increased. Although the adsorption performance of biochars decreased as the pH increased, both CBC-800 and PBC-800 also possessed considerable adsorption capacities of 160.6 and 164.4 mg/g, respectively. This demonstrated that CBC-800 and PBC-800 were capable of effectively adsorbing PFOA across a wide pH range.

The adsorption of PFOA by biochar was also influenced by the presence of ions in the solution, except pH. The impact of co-existing Na⁺ and Ca²⁺ ions at varying concentrations on the porous biochar adsorption performances is illustrated in [Figure 4B](#) and [C](#). It was observed that the adsorption performance of porous biochars increased as the concentrations of Na⁺ and Ca²⁺ increased. This was due to the fact that the compressed double electric layer effect resulted in a decrease in the negative charge of biochars, thus weakening the electrostatic repulsion between biochars and PFOA molecules (and between the adsorbed PFOA anion)^[42]. In comparison with Na⁺, Ca²⁺ demonstrated a more pronounced enhancement of the adsorption capacities of biochars for PFOA, with this effect becoming more evident at higher Ca²⁺ concentrations. PFOA molecules contained carboxyl groups, while the surface of biochar contained hydroxyl and carboxyl functional groups [[Supplementary Figure 3A](#)]. Ca²⁺ could serve as a bridge bond between the deprotonated PFOA molecules and the functional groups of biochars, thereby promoting the adsorption of PFOA^[43]. The influence of NO₃[–] and SO₄^{2–} on the adsorption of PFOA by biochar was investigated [[Supplementary Figure 4](#)]. As the concentrations of NO₃[–] and SO₄^{2–} increased from 0 to 50 mM, the adsorption of PFOA by biochar was significantly enhanced. This increase was mainly due to the salting-out effects^[34]. Furthermore, it was observed that the enhancement of Na₂SO₄ for adsorption was lower than NaNO₃. This may be due to the fact that SO₄^{2–} was more likely to compete with PFOA for adsorption sites on biochar^[44].

To validate the application of CBC-800 in relevant environment concentrations, an adsorption experiment was conducted at low concentrations (10–1,000 µg/L) [[Figure 5A](#)]. The results demonstrated that CBC-800 exhibited an excellent removal rate (87.4%) even at an initial concentration of 10 µg/L. Furthermore, the removal efficiency of CBC-800 exhibited a positive correlation with the initial concentration. This was due to that at higher concentrations, there was a larger mass transfer driving force. This meant that the concentration gradient between the bulk solution and the adsorbent surface is greater, which facilitates the

Table 3. Thermodynamic parameters of adsorption of PFOA by biochars

Biochars	T (K)	Freundlich			ΔG^0 (kJ/mol)	ΔH^0 (kJ/mol)	ΔS^0 (J·mol ⁻¹ ·K ⁻¹)
		K_f (mg ¹⁻ⁿ ·g ⁻¹ ·L ⁿ)	n	R ²			
PBC-800	288	102.11 ± 5.67	0.30 ± 0.01	0.994	-11.08	-9.20	5.92
	298	71.89 ± 10.16	0.35 ± 0.03	0.975	-10.59		
	308	79.97 ± 6.55	0.26 ± 0.02	0.982	-11.22		
CBC-800	288	170.38 ± 23.47	0.25 ± 0.03	0.956	-12.30	-18.30	-20.61
	298	141.67 ± 8.93	0.28 ± 0.01	0.991	-12.27		
	308	103.57 ± 13.77	0.33 ± 0.03	0.974	-11.88		

PFOA: Perfluorooctanoic acid; PBC: pine sawdust-modified biochars; CBC: corn stalks-modified biochars.

movement of PFOA molecules toward the biochar. This leads to an increased rate of adsorption, as the molecules are more likely to collide with and adhere to the biochar surface. However, at lower concentrations, this concentration gradient is much smaller, resulting in a reduced driving force for adsorption and fewer collisions between PFOA molecules and the biochar surface^[45]. A recycling experiment was performed to assess the long-term adsorption performance of CBC-800 for PFOA at a concentration of 40 µg/L [Figure 5B]. The results indicated the removal rate of CBC-800 (93.4%–94.5%) did not significantly decline even at six consecutive adsorption cycles. The above findings showed CBC-800 had excellent consecutive adsorption performance at low concentrations of PFOA, making it able to effectively remediate the PFOA-contaminated water.

Adsorption stability was regarded as a key factor for practical application and economic feasibility. The adsorption stability was evaluated through a desorption experiment. PFOA adsorbed on porous biochars was desorbed using DIW, 0.5 M NaOH, and different concentrations of ethanol. As illustrated in Figure 5C, CBC-800 and PBC-800 exhibited low PFOA desorption rates in 0.5 M NaOH (3.6% and 7.4%) and DIW (19.6% and 25.9%), demonstrating CBC-800 and PBC-800 owned excellent adsorption stability for PFOA. The lower desorption rate of CBC-800 was consistent with the result that CBC-800 showed a stronger combination than PBC-800 according to the ΔS^0 values of adsorption thermodynamics. Additionally, the PFOA desorption rates of CBC-800 and PBC-800 in ethanol (25%–95%) ranged from 75.5% to 95.1% and 79.4% to 93.2%, respectively, suggesting that low concentrations of ethanol could be effective for biochar regeneration.

Adsorption mechanisms

The adsorption mechanisms of PFOA on adsorbents primarily included hydrophobic interaction, pore filling, electrostatic interaction, and hydrogen bonding^[41]. In this study, the porous biochar exhibited notable adsorption performance for PFOA. However, the adsorption mechanisms between KHCO₃-modified biochar and PFOA remained unclear.

Hydrophobic interaction was expected to follow a linear isotherm, with the Freundlich nonlinearity factor (n) approaching 1, showing that more hydrophobic interactions were involved in the adsorption of biochars. However, the nonlinearity factor n (0.26–0.35) for all biochars was relatively low, suggesting that hydrophobic interaction was not important for the adsorption of PFOA by porous biochars. Pore filling was a crucial mechanism in PFOA adsorption^[46]. The porous biochars had an average pore size of greater than 1.9 nm [Table 1], which allowed PFOA molecules, with a size of approximately 1.1 nm [Supplementary Table 1], to enter their pore structure. Furthermore, the Pearson correlation coefficient (R²) between the Q_m of biochars obtained from the Langmuir model [Supplementary Table 3] and the physical properties of biochars [Table 1] showed a strong positive correlation between Q_m and both the S_{BET} and S_{mic} , indicating

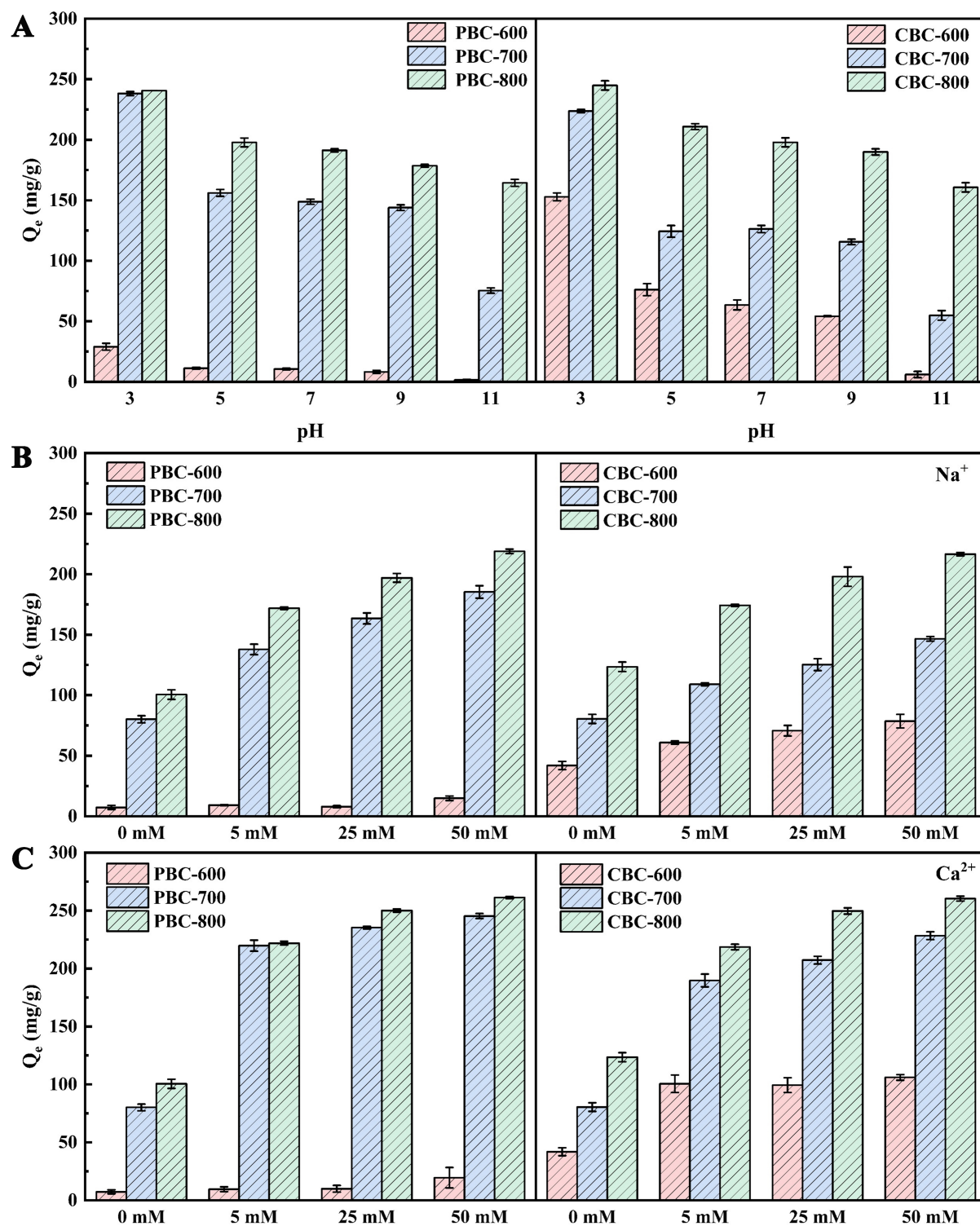


Figure 4. Effect of (A) pH, (B) Na^+ , and (C) Ca^{2+} ions on the adsorption of PFOA by biochars. PFOA: Perfluorooctanoic acid.

that biochar adsorption capacity was greatly impacted by the pore structure [Figure 5D]. Therefore, pore filling was the dominant adsorption mechanism. For electrostatic interaction, the zeta potential of all biochars was consistently negative across the pH range of 3–11 [Supplementary Figure 5]. Given that the

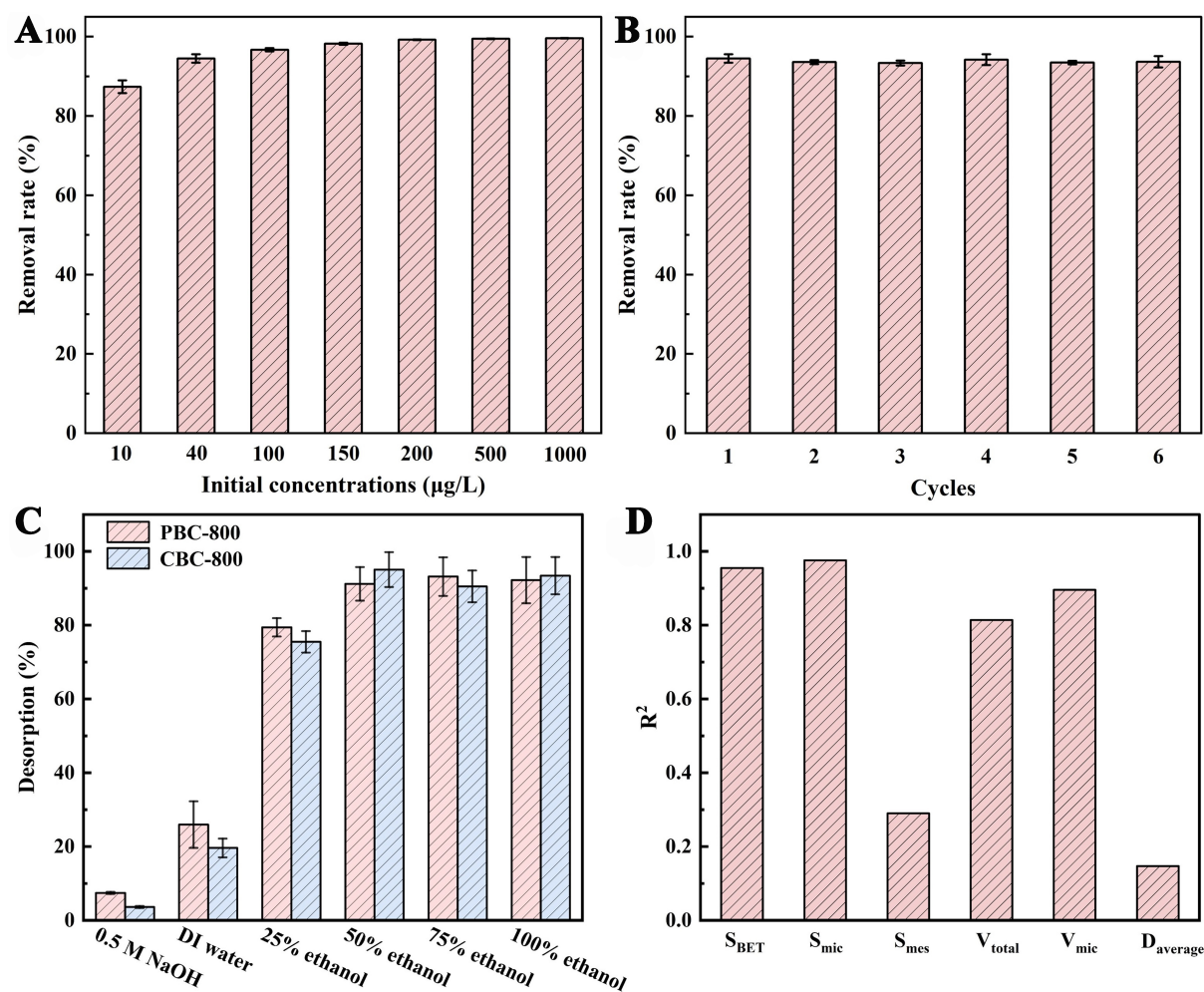


Figure 5. (A) The removal rate of CBC-800 for different initial concentrations; (B) the adsorption cycles of CBC-800 for low concentration of PFOA; (C) PFOA desorption by different desorption solutions and (D) correlation coefficient between the physical properties of biochars and the maximum adsorption capacity (Q_m). CBC: Corn stalks-modified biochars; PFOA: perfluorooctanoic acid.

pKa of PFOA was 1.3, the hydrophilic head of PFOA existed as negatively charged ions when $pH > pKa$ ^[47]. Consequently, as pH increased, electrostatic repulsion between the biochar and PFOA increased, leading to a decrease in biochar adsorption capacity [Figure 4A]. Therefore, electrostatic interaction significantly affected the PFOA adsorption by biochars. The -COOH and -OH functional groups on biochar enabled it to serve as a hydrogen donor. Simultaneously, the deprotonation of carboxyl groups at the head of PFOA molecules facilitates their role as hydrogen acceptors^[48]. By comparing the FTIR of biochars before and after PFOA adsorption [Supplementary Figure 3A and B], the -OH of biochars ($3,420\text{ cm}^{-1}$) showed no obvious difference, indicating that hydrogen bonding interaction was not the dominant adsorption mechanism.

In summary, $KHCO_3$ modification significantly increased the S_{BET} of the biochar, resulting in pore filling dominating the PFOA adsorption, and electrostatic interaction played an important role, while hydrogen bonding and hydrophobic interaction also existed, as illustrated in Figure 6.

These findings demonstrated that the $KHCO_3$ modification can significantly enhance the surface properties of the biochar, improving its adsorption capacity for PFOA. $KHCO_3$ is a relatively mild pore-enlarging

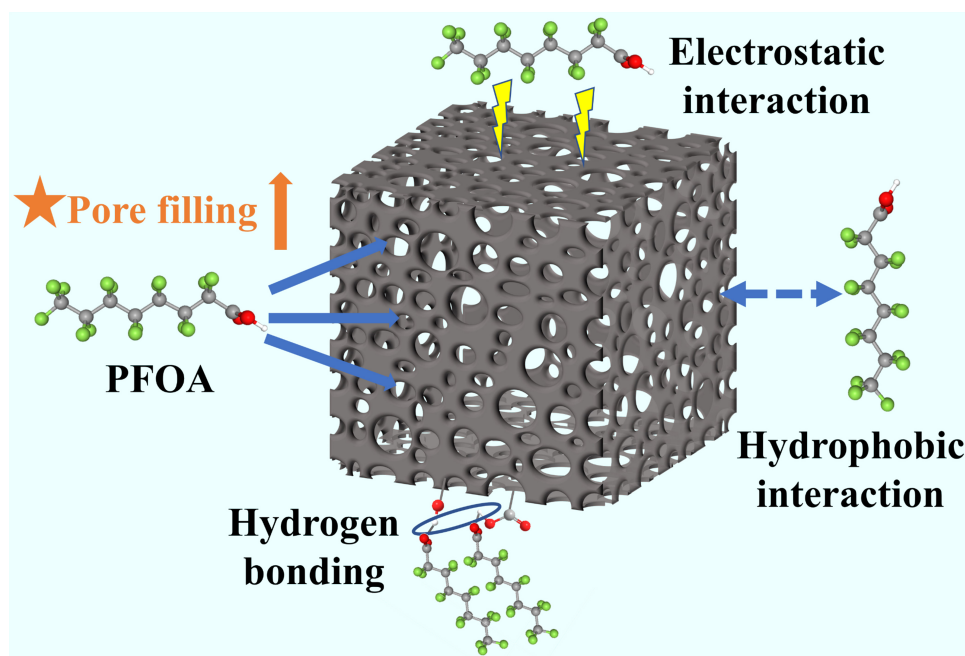


Figure 6. Schematic mechanism of PFOA adsorption on porous biochar. PFOA: Perfluorooctanoic acid.

reagent with minimal environmental impact, making the production of modified biochar economically viable for large-scale water treatment applications^[19]. Additionally, the porous biochar could be regenerated with a low concentration of ethanol, which can reduce the overall cost. However, the modification also had some disadvantages. For example, although KHCO_3 -modified biochar may effectively adsorb PFOA, it may also adsorb other contaminants present in the water^[49], leading to competition and reduced efficiency in specific PFOA removal. Organic matter in water, such as HA, may interact with the biochar, and the part adsorption sites were occupied^[24], leading to a decrease in the adsorption capacity. While KHCO_3 -modified biochar presented a promising solution for PFOA removal, careful consideration of its advantages and disadvantages is essential for its effective application in environmental remediation strategies.

CONCLUSIONS

In this study, low-cost and environmentally friendly porous biochar was successfully prepared by pyrolyzing corn stalks and pine sawdust with KHCO_3 as a green activator. The resulting biochar, CBC-800, demonstrated more graphite defects and a higher SSA, which provide fast diffusion channels for the diffusion of PFOA, thereby promoting the adsorption of PFOA. The adsorption of PFOA on CBC-800 was fast and efficient, with the maximum adsorption capacity, as obtained by the Langmuir model, reaching 514.8 mg/g, which was advantageous over other adsorbents. The adsorption kinetic and isotherm data were better fitted by the pseudo-second-order kinetics and Freundlich models, respectively, indicating that chemisorption was the rate-limiting stage in the adsorption process. Thermodynamic results demonstrated that the adsorption process was both physically spontaneous and exothermic. CBC-800 demonstrated a high adsorption capacity for PFOA across a wide pH range and in the presence of various ions. Furthermore, the removal rate of low concentrations experiments demonstrated that CBC-800 had excellent consecutive adsorption performance at low PFOA concentrations. The adsorption mechanism study provided that pore filling was identified as the dominant adsorption mechanism. Given the superior adsorption capacity and low environmental impact of CBC-800, KHCO_3 -modified biochar has a promising potential application in practical water-contaminated environments and wastewater treatment processes to remove PFOA and contribute to environmental protection.

DECLARATIONS

Authors' contributions

Formal analysis, investigation, conceptualization, data curation, writing - original draft, visualization: Hu, T.

Conceptualization, writing - review and editing, formal analysis: Wu, J. Q.

Methodology, formal analysis, data curation: Wang, T. S.

Resources, formal analysis: Li, S. J.

Resources, conceptualization, writing-review and editing, supervision, project administration, funding acquisition: Chen, J. W.

Availability of data and materials

The raw data supporting the findings of this study are available within this Article and its [Supplementary Materials](#). Further data are available from the corresponding author upon reasonable request.

Financial support and sponsorship

This study was supported by the National Natural Science Foundation of China (41731282).

Conflicts of interest

Chen, J. W. is the Guest Editor of the Special Issue "Research Advances in the Control and Removal Strategies for PFAS Contaminants" and an Editorial Board member of the journal *Water Emerging Contaminants & Nanoplastics*. Chen, J. W. was not involved in any steps of editorial processing, notably including reviewer selection, manuscript handling, and decision making. The other authors declared that there are no conflicts of interest.

Ethical approval and consent to participate

Not applicable.

Consent for publication

Not applicable.

Copyright

© The Author(s) 2025.

REFERENCES

1. Kucharzyk, K. H.; Darlington, R.; Benotti, M.; Deeb, R.; Hawley, E. Novel treatment technologies for PFAS compounds: a critical review. *J. Environ. Manage.* **2017**, *204*, 757-64. [DOI](#) [PubMed](#)
2. Wang, J.; Cao, C.; Wang, Y.; Wang, Y.; Sun, B.; Zhu, L. In situ preparation of *p-n* BiOI@Bi₅O₇I heterojunction for enhanced PFOA photocatalytic degradation under simulated solar light irradiation. *Chem. Eng. J.* **2020**, *391*, 123530. [DOI](#)
3. Lang, J. R.; Allred, B. M.; Field, J. A.; Levis, J. W.; Barlaz, M. A. National estimate of per- and polyfluoroalkyl substance (PFAS) release to U.S. municipal landfill leachate. *Environ. Sci. Technol.* **2017**, *51*, 2197-205. [DOI](#) [PubMed](#)
4. Evich, M. G.; Davis, M. J. B.; McCord, J. P.; et al. Per- and polyfluoroalkyl substances in the environment. *Science* **2022**, *375*, eabg9065. [DOI](#) [PubMed](#) [PMC](#)
5. Houtz, E. F.; Higgins, C. P.; Field, J. A.; Sedlak, D. L. Persistence of perfluoroalkyl acid precursors in AFFF-impacted groundwater and soil. *Environ. Sci. Technol.* **2013**, *47*, 8187-95. [DOI](#) [PubMed](#)
6. Yu, H.; Chen, H.; Zhang, P.; et al. In situ self-sacrificial synthesis of polypyrrole/biochar composites for efficiently removing short- and long-chain perfluoroalkyl acid from contaminated water. *J. Environ. Manage.* **2023**, *344*, 118745. [DOI](#)
7. Tian, D.; Geng, D.; Tyler, M. W.; et al. Removal of perfluorooctanoic acid (PFOA) from aqueous solution by amino-functionalized graphene oxide (AGO) aerogels: Influencing factors, kinetics, isotherms, and thermodynamic studies. *Sci. Total. Environ.* **2021**, *783*, 147041. [DOI](#)
8. Zeng, Z.; Song, B.; Xiao, R.; et al. Assessing the human health risks of perfluorooctane sulfonate by in vivo and in vitro studies.

- Environ. Int.* **2019**, *126*, 598-610. DOI
9. Chen, Z.; Liu, Y.; Wei, W.; Ni, B. Recent advances in electrocatalysts for halogenated organic pollutant degradation. *Environ. Sci. Nano.* **2019**, *6*, 2332-66. DOI
 10. Luo, P.; Zhang, Y.; Peng, Z.; et al. Photocatalytic degradation of perfluorooctanoic acid (PFOA) from water: a mini review. *Environ. Pollut.* **2024**, *343*, 123212. DOI
 11. Singh, M.; Ahsan, M.; Pandey, V.; et al. Comparative assessment for removal of anionic dye from water by different waste-derived biochar vis a vis reusability of generated sludge. *Biochar* **2022**, *4*, 140. DOI
 12. Deng, S.; Chen, J.; Chang, J. Application of biochar as an innovative substrate in constructed wetlands/biofilters for wastewater treatment: performance and ecological benefits. *J. Clean. Prod.* **2021**, *293*, 126156. DOI
 13. Zhang, X.; Tian, J.; Wang, P.; et al. Highly-efficient nitrogen self-doped biochar for versatile dyes' removal prepared from soybean cake via a simple dual-templating approach and associated thermodynamics. *J. Clean. Prod.* **2022**, *332*, 130069. DOI
 14. Zhang, J.; Chen, Z.; Liu, Y.; Wei, W.; Ni, B. Removal of emerging contaminants (ECs) from aqueous solutions by modified biochar: a review. *Chem. Eng. J.* **2024**, *479*, 147615. DOI
 15. He, J.; Gomeniuc, A.; Olshansky, Y.; et al. Enhanced removal of per- and polyfluoroalkyl substances by crosslinked polyaniline polymers. *Chem. Eng. J.* **2022**, *446*, 137246. DOI
 16. Yu, H.; Zhang, P.; Chen, H.; et al. Porous polypyrrole with a vesicle-like structure for efficient removal of per- and polyfluoroalkyl substances from water: crucial role of porosity and morphology. *J. Hazard. Mater.* **2024**, *462*, 132748. DOI
 17. Fagbayigbo, B. O.; Opeolu, B. O.; Fatoki, O. S.; Akenga, T. A.; Olatunji, O. S. Removal of PFOA and PFOS from aqueous solutions using activated carbon produced from *Vitis vinifera* leaf litter. *Environ. Sci. Pollut. Res. Int.* **2017**, *24*, 13107-20. DOI PubMed
 18. Deng, S.; Nie, Y.; Du, Z.; et al. Enhanced adsorption of perfluorooctane sulfonate and perfluorooctanoate by bamboo-derived granular activated carbon. *J. Hazard. Mater.* **2015**, *282*, 150-7. DOI
 19. Cheng, H.; Bian, Y.; Wang, F.; et al. Green conversion of crop residues into porous carbons and their application to efficiently remove polycyclic aromatic hydrocarbons from water: sorption kinetics, isotherms and mechanism. *Bioresour. Technol.* **2019**, *284*, 1-8. DOI
 20. Wang, W.; Lin, J.; Shao, S.; Chen, H.; Dai, J.; Yang, Y. Enhanced adsorption of benzo(a)pyrene in soil by porous biochar: adsorption kinetics, thermodynamics, and mechanisms. *J. Environ. Chem. Eng.* **2023**, *11*, 109002. DOI
 21. Ma, P.; Yao, S.; Wang, Z.; Qi, F.; Liu, X. Preparation of nitrogen-doped hierarchical porous carbon aerogels from agricultural wastes for efficient pollution adsorption. *Sep. Purif. Technol.* **2023**, *311*, 123250. DOI
 22. Jing, F.; Guan, J.; Tang, W.; Chen, J. Mechanistic insight into adsorptive removal of ionic NOR and nonionic DEP organic contaminants by clay-biochar composites. *Environ. Pollut.* **2022**, *310*, 119881. DOI
 23. Wang, T.; Wu, J.; Hu, T.; et al. Mechanistic insights into adsorption-desorption of PFOA on biochars: effects of biomass feedstock and pyrolysis temperature, and implication of desorption hysteresis. *Sci. Total. Environ.* **2024**, *957*, 177668. DOI
 24. Wang, K.; Wang, Y.; Zhang, S.; Chen, Y. D.; Wang, R.; Ho, S. H. Tailoring a novel hierarchical cheese-like porous biochar from algae residue to boost sulfathiazole removal. *Environ. Sci. Ecotechnol.* **2022**, *10*, 100168. DOI PubMed PMC
 25. Ouyang, T.; Zhang, T.; Wang, H.; et al. High-throughput fabrication of porous carbon by chemical foaming strategy for high performance supercapacitor. *Chem. Eng. J.* **2018**, *352*, 459-68. DOI
 26. Asadullah, M.; Asaduzzaman, M.; Kabir, M. S.; Mostofa, M. G.; Miyazawa, T. Chemical and structural evaluation of activated carbon prepared from jute sticks for Brilliant Green dye removal from aqueous solution. *J. Hazard. Mater.* **2010**, *174*, 437-43. DOI PubMed
 27. Li, X.; Huang, Y.; Liang, X.; et al. Characterization of biochars from woody agricultural wastes and sorption behavior comparison of cadmium and atrazine. *Biochar* **2022**, *4*, 132. DOI
 28. Zhu, H.; Liu, X.; Jiang, Y.; Lin, D.; Yang, K. Sorption kinetics of 1,3,5-trinitrobenzene to biochars produced at various temperatures. *Biochar* **2022**, *4*, 157. DOI
 29. Wu, J.; Wang, T.; Liu, Y.; Tang, W.; Geng, S.; Chen, J. Norfloxacin adsorption and subsequent degradation on ball-milling tailored N-doped biochar. *Chemosphere* **2022**, *303*, 135264. DOI
 30. Tang, W.; Jing, F.; Laurent, Z. B. L. G.; Liu, Y.; Chen, J. High-temperature and freeze-thaw aged biochar impacts on sulfonamide sorption and mobility in soil. *Chemosphere* **2021**, *276*, 130106. DOI
 31. Xu, Q.; Liu, T.; Li, L.; et al. Hydrothermal carbonization of distillers grains with clay minerals for enhanced adsorption of phosphate and methylene blue. *Bioresour. Technol.* **2021**, *340*, 125725. DOI
 32. Yang, Y.; Luo, X.; Zhang, J.; Ma, X.; Sun, P.; Zhao, L. Sewage sludge-coconut fiber co-pyrolysis biochar: mechanisms underlying synergistic heavy metal stabilization and ciprofloxacin adsorption. *J. Clean. Prod.* **2022**, *375*, 134149. DOI
 33. Kan, T.; Strezov, V.; Evans, T.; et al. Catalytic pyrolysis of biomass impregnated with elements from steelmaking slag leaching and simultaneous fabrication of phosphorus adsorbent. *J. Clean. Prod.* **2021**, *328*, 129490. DOI
 34. Lei, X.; Yao, L.; Lian, Q.; et al. Enhanced adsorption of perfluorooctanoate (PFOA) onto low oxygen content ordered mesoporous carbon (OMC): adsorption behaviors and mechanisms. *J. Hazard. Mater.* **2022**, *421*, 126810. DOI
 35. Li, Y.; Shang, H.; Cao, Y.; Yang, C.; Feng, Y.; Yu, Y. High performance removal of sulfamethoxazole using large specific area of biochar derived from corncob xylose residue. *Biochar* **2022**, *4*, 128. DOI
 36. Velusamy, K.; Periyasamy, S.; Kumar, P. S.; et al. Analysis on the removal of emerging contaminant from aqueous solution using biochar derived from soap nut seeds. *Environ. Pollut.* **2021**, *287*, 117632. DOI
 37. Wang, B.; Jiang, Y. S.; Li, F. Y.; Yang, D. Y. Preparation of biochar by simultaneous carbonization, magnetization and activation for norfloxacin removal in water. *Bioresour. Technol.* **2017**, *233*, 159-65. DOI

38. Ma, Y.; Li, M.; Li, P.; et al. Hydrothermal synthesis of magnetic sludge biochar for tetracycline and ciprofloxacin adsorptive removal. *Bioresour. Technol.* **2021**, *319*, 124199. DOI
39. Heo, J.; Yoon, Y.; Lee, G.; Kim, Y.; Han, J.; Park, C. M. Enhanced adsorption of bisphenol A and sulfamethoxazole by a novel magnetic CuZnFe₂O₄-biochar composite. *Bioresour. Technol.* **2019**, *281*, 179-87. DOI
40. Wang, G.; Yong, X.; Luo, L.; Yan, S.; Wong, J. W.; Zhou, J. Structure-performance correlation of high surface area and hierarchical porous biochars as chloramphenicol adsorbents. *Sep. Purif. Technol.* **2022**, *296*, 121374. DOI
41. Yea, Y.; Kim, G.; Wang, D.; et al. Selective sequestration of perfluorinated compounds using polyaniline decorated activated biochar. *Chem. Eng. J.* **2022**, *430*, 132837. DOI
42. Qian, J.; Martinez, A.; Marek, R. F.; et al. Polymeric nanofiber-carbon nanotube composite mats as fast-equilibrium passive samplers for polar organic contaminants. *Environ. Sci. Technol.* **2020**, *54*, 6703-12. DOI
43. Liu, Z.; Zhang, P.; Wei, Z.; et al. Porous Fe-doped graphitized biochar: an innovative approach for co-removing per-/polyfluoroalkyl substances with different chain lengths from natural waters and wastewater. *Chem. Eng. J.* **2023**, *476*, 146888. DOI
44. Lei, X.; Lian, Q.; Zhang, X.; et al. Removal of perfluorooctanoic acid via polyethyleneimine modified graphene oxide: effects of water matrices and understanding mechanisms. *Chemosphere* **2022**, *308*, 136379. DOI
45. Sekulic M, Boskovic N, Milanovic M, Grujic Letic N, Gligoric E, Pap S. An insight into the adsorption of three emerging pharmaceutical contaminants on multifunctional carbonous adsorbent: mechanisms, modelling and metal coadsorption. *J. Mol. Liq.* **2019**, *284*, 372-82. DOI
46. Heidari, H.; Abbas, T.; Ok, Y. S.; Tsang, D. C. W.; Bhatnagar, A.; Khan, E. GenX is not always a better fluorinated organic compound than PFOA: a critical review on aqueous phase treatability by adsorption and its associated cost. *Water. Res.* **2021**, *205*, 117683. DOI
47. Fang, J.; Xu, K.; Liu, A.; et al. Selective perfluorooctanoic acid (PFOA) and perfluorooctane sulfonate (PFOS) adsorption by nanoscale zero-valent iron (nZVI): performance and mechanisms. *Environ. Sci. Nano.* **2024**, *11*, 1915-25. DOI
48. Wang, M.; Orr, A. A.; Jakubowski, J. M.; et al. Enhanced adsorption of per- and polyfluoroalkyl substances (PFAS) by edible, nutrient-amended montmorillonite clays. *Water. Res.* **2021**, *188*, 116534. DOI PubMed PMC
49. Truong, Q. M.; Nguyen, T. B.; Chen, C. W.; Chen, W. H.; Bui, X. T.; Dong, C. D. KHCO₃-activated high surface area biochar derived from brown algae: a case study for efficient adsorption of Cr(VI) in aqueous solution. *Environ. Res.* **2024**, *247*, 118227. DOI